First-principles studies of structural, electronic, and dynamical properties of Be chalcogenides

G. P. Srivastava,[1] H. M. Tütüncü,[2] and N. Günhan[2]

[1]*School of Physics, University of Exeter, Stocker Road, Exeter EX4 4QL, United Kingdom*
[2]*Sakarya Üniversitesi, Fen-Edebiyat Fakültesi, Fizik Bölümü, Adapazarı, Turkey*

We have studied structural, electronic, and dynamical properties of Be chalcogenides (BeS, BeSe, and BeTe) by employing the plane-wave pseudopotential method within the density functional theory. The calculated lattice constant and bulk modulus for these compounds are found to be in good agreement with previous theoretical and experimental results. The electronic band structure is also presented for these materials. In particular, the calculated electronic valence band structure for BeTe shows very good agreement with an angle-resolved synchrotron-radiation photoemission spectroscopy data along the [100] direction. Phonon dispersion curves and density of states were calculated by employing a density-functional perturbation theory. It is found that the dispersion characteristics of the optical branches in these materials are very different from those of any other II-VI materials. An explanation of these characteristics is forwarded in terms of the large mass difference between Be and the chalcogens.

I. INTRODUCTION

II-VI materials are characterized by different degrees of covalent, ionic, and metallic bonding and thus offer a wide range of physical properties. For example, these materials can crystalize with different crystal structures (such as zinc-blende and wurtzite), and can exhibit a wide range of electronic band gap (such as semimetallic for HgTe and in the UV range for ZnS). Recently, there has been great interest in the study of structural and electronic properties of beryllium chalcogenides (BeS, BeSe, and BeTe).[1–9] These materials are promising semiconductors for light emitting optoelectronics devices in the blue colour spectrum[6] with large direct band gap. In addition to this, these semiconductors are potentially a good choice for technological applications due to their hardness.[2] Thus, several attempts have been made to investigate the structural, electronic properties of zinc-blende phases of Be-chalcogenide materials. Few experimental data are available for the electronic structures of these materials due probably to difficulty in growing single crystals or good quality epitaxial layers.[6,8] In particular, the dispersion of the top valence bands of BeTe along the Γ-X direction has been measured using angle-resolved synchrotron-radiation photoemission spectroscopy.[8] On the theoretical side, a first-principles pseudopotential method has been used to investigate structural and electronic properties of the zinc-blende phase of Be-chalcogenide materials.[3–5,7,8] The all-electron full-potential linear augmented-plane wave method has been employed to structural and electronic properties of BeS.[9]

Although considerable progress has been made in theoretical description of the structural and electronic properties of Be-chalcogenide materials, many of their vibrational properties are still not well established. An accurate description of vibrational properties of solids is important, as these play a significant role in determining various material properties such as phase transition, electron-phonon interactions, and transport coefficients. Due to the very low mass of Be, lattice dynamical properties of Be chalcogenides are expected to exhibit extraordinary features. Recently, the simple phenom-

enological De Launey model,[10] based on a reduced number of central and angular force constants, has been applied by Doyen-Lang *et al.*[11] to calculate the phonon dispersion curves of BeSe and BeTe. First-principles calculations, based on the frozen-phonon approximation within the pseudopotential method and the density functional scheme, have been reported for the zone-center TO phonon frequency in BeSe and BeTe.[12,13] The first-principles results for the zone-center TO mode, as expected, are in very good agreement with experimentally determined values[12,13] obtained from Raman and infrared spectroscopies.

The aim of the present work is to investigate structural, electronic, and dynamical properties of Be-chalcogenide materials by employing the plane-wave pseudopotential method, density functional theory, and a linear response technique. The calculated structural parameters are compared with previous theoretical calculations and available experimental results. In particular, the calculated electronic band structure for BeTe shows very good agreement with experimental results[8] for the top valence bands along the Γ-X direction. The calculated phonon results are also compared with available experimental and theoretical results. It is pointed out that compared with other zinc-blende semiconductors, the dispersion of the TO and LO branches are rather peculiar. An explanation for these peculiarities are forwarded in terms of the large mass difference between Be and the chalcogens.

II. METHOD

We have used a first-principles pseudopotential method based on the density functional theory within the local-density approximation. We employed norm-conserving pseudopotentials to treat the interaction between valence electrons and ions. The pseudopotentials were generated by adopting the scheme described by Troullier and Martins.[14] For generating the Be pseudopotentials we included the non-linear core correction. In dealing with electron-electron inter-

TABLE I. Lattice constant a_o, bulk modulus B, the pressure derivative of bulk modulus B′ and macroscopic dielectric constant ε_∞ of the zinc-blende phase of BeS, BeSe, and BeTe. The presently calculated results are compared with other theoretical and experimental data.

Material	Reference	a_0(Å)	B (Mbar)	B′(Mbar)	ε_∞
BeS	Present	4.81	0.93	3.34	5.46
	Theory[a]	4.82	1.13	3.99	
	Theory[b]	4.77	1.16		
	Theory[c]	4.77	1.02		
	Theory[d]	4.75	1.16	3.22	
	Experimental[e]	4.86			
BeSe	Present	5.13	0.80	3.56	6.09
	Theory[b]	5.04	0.98		
	Theory[d]	5.04	0.98	3.11	
	Experimental	5.14[f]	0.92[f]		6.1[g]
BeTe	Present	5.58	0.60	3.72	7.51
	Theory[b]	5.53	0.70		
	Theory[d]	5.53	0.71	3.38	
	Experimental[f]	5.62	0.67		
	Experimental[h]				7.00

[a]Reference 9.
[b]Reference 7.
[c]Reference 5.
[d]Reference 3.
[e]Reference 24.
[f]Reference 25.
[g]Reference 13.
[h]Reference 12.

action we employed the Ceperley-Alder form of the exchange and correlation potentials, as parametrized by Perdew and Zunger.[15] The Kohn-Sham single-particle functions were expanded in a basis of plane waves. Self-consistent solutions of the Kohn-Sham equations were obtained by sampling the irreducible part of the Brillouin zone by employing special **k**-points.[16] Well-converged results were obtained for the lattice constant and bulk modulus of the three chalogenide materials with the consideration of the kinetic energy cutoff of 40 Ry, and ten special **k**-points. Having obtained self-consistent solutions of the Kohn-Sham equations, phonon dispersion curves were calculated by using the perturbative response computer program described by Baroni *et al.*[17] In particular, eight dynamical matrices were calculated for a $n \times n \times n$ phonon **q**-points mesh within the irreducible part of the Brillouin zone. These matrices were then Fourier-interpolated to obtain the phonon dispersion curves and density of states. Tests with different sets of the **q**-points mess indicated that calculated phonon frequencies converged to better than 4 cm^{-1} for the $4 \times 4 \times 4$ **q**-points mesh.

III. RESULTS

A. Convergence tests

Convergence with respect to the kinetic energy cut-off E_c and special **k**-points was tested against the calculated results for the various quantities, such as the equilibrium lattice constant a, bulk modulus B, the pressure derivative of bulk modulus B', band gap at the zone center $E_g(\Gamma)$, macroscopic dielectric constant ε_∞, and the zone center optical frequencies TO(Γ), and LO(Γ). With 10 special **k**-points, the results for [a(Å), B(Mbar), B', TO(Γ) (cm^{-1}), LO(Γ) (cm^{-1}), ε_∞, $E_g(\Gamma)$(eV)] ranged from (4.820, 0.955, 3.222, 557.08, 646.44, 5.769, 5.548) for $E_c=20$ Ry to (4.816, 0.925, 3.384, 562.14, 648.22, 5.906, 5.378) for $E_c=50$ Ry. Similarly, for $E_c=40$ Ry the results for [a(Å), B(Mbar), B', TO(Γ) (cm^{-1}), LO(Γ) (cm^{-1}), ε_∞, $E_g(\Gamma)$(eV)] ranged from (4.816, 0.931, 3.274, 561.97, 648.33, 5.896, 5.3856) for 10 **k**-points to (4.814, 0.926, 3.338, 562.65, 647.17, 5.458, 5.389) for 84 **k**-points. Thus we conclude that the results are well converged for the choice 40 Ry and 10 **k**-points. Converged values of a, B, B', and ε_∞ for BeS, BeSe, and BeTe are presented in Table I.

B. Structural and electronic properties

The equilibrium lattice parameter has been calculated by minimizing the crystal total energy calculated for different values of the lattice constant with the help of Murnaghan's equation of state. The calculated values of the cubic lattice constant for BeS, BeSe and BeTe are 4.81, 5.13, and 5.58 Å, respectively. These values compare quite well with the experimentally obtained values[18] of 4.86, 5.14, and 5.63 Å, respectively. The agreement with the available experimental
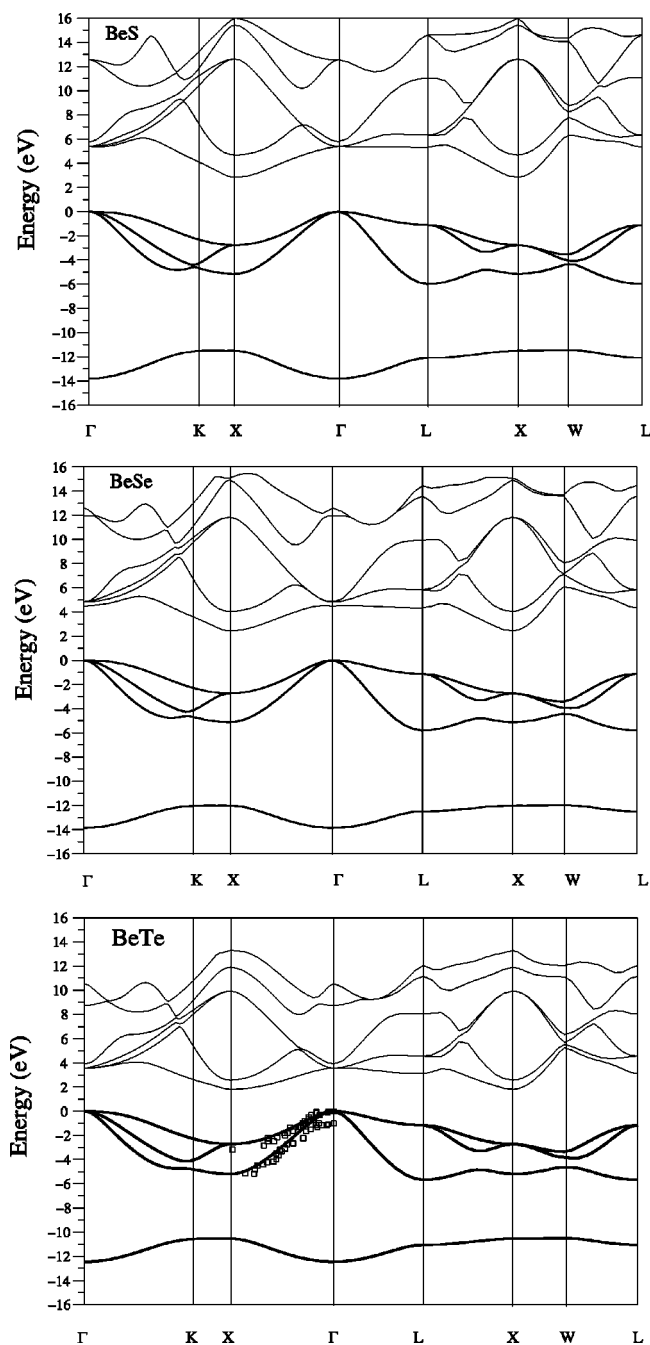
FIG. 1. Calculated electronic band structures of Be chalcogenides. The obtained valence band dispersion for BeTe along the [100] direction are compared with experimental measurements (Ref. 3). The theory does not include spin-orbit interaction, and thus comparison between the calculated and experimental dispersion curves should not be made near the zone center.

and theoretical results for B and B' is also good. In addition to these parameters, we have presented the optical dielectric constants of these materials in this table. The calculated optical dielectric constant results of 6.09(7.51) for BeSe(BeTe) compare well with experimental values 6.1(7.0).[12,13]

Figure 1 displays our calculated electronic band structures for BeS, BeSe, and BeTe along the high-symmetry directions. All these materials are characterized by an indirect

TABLE II. The calculated electronic band gaps for the zinc-blende phase of BeS, BeSe, and BeTe, and their comparison with other theoretical and experimental data.

Material	Reference	Direct (at Γ)	Indirect ($\Gamma-X$)
BeS	Present	5.39	2.83
	Theory[a]	5.51	2.75
	Theory[b]	5.39	2.81
	Theory[c]		4.17
	Theory[d]	5.50	2.84
BeSe	Present	4.50	2.43
	Theory[a]	4.72	2.39
	Theory[c]		3.61
BeTe	Present	3.57	1.80
	Theory[a]	3.68	1.80
	Expt.[e]	1.45	2.89
	Expt.[f]	4.53	

[a]Reference 7.
[b]Reference 5.
[c]Reference 1.
[d]Reference 9.
[e]Reference 24.
[f]Reference 8.

band gap along the Γ-X direction, with the minimum of the conduction band lying at the X point. The direct and indirect band gap results are listed in Table II. Of the three materials, BeTe exhibits the smallest values of the direct and indirect band gaps. For BeTe the calculated direct and indirect band gap results of 3.57 and 1.80 eV, respectively, are much smaller than the experimental values of 4.53 and 2.80 eV,[8] respectively. Such reduction in calculated band gaps, within the local density approximation, is well understood,[19] and it is expected that a quasiparticle calculation will bring in reasonable agreement between theory and experiment.

The calculated results for BeTe show very good agreement with experimental results for the top valence bands along the Γ-X direction. We point out that the experimental results for BeTe show a significant amount of spin-orbit interaction at the zone center. Our calculations do not include this interaction, and consequently we cannot compare our theoretical results with experiment near the zone center.

C. Phonon dispersion curves and density of states

The calculated phonon dispersion curves and the density of states curves are presented in Fig. 2. Our calculated results are compared with available theoretical and experimental results in Table III. A few trends can be established across BeS, BeSe, and BeTe. Denoting M_{Be} and M_{ch} as beryllium and chalcogen masses, respectively, we find that the width of the acoustic frequency range varies as $1/\sqrt{M_{ch}}$, and the optical-acoustic gap varies as $(1-\sqrt{M_{Be}/M_{ch}})$, in accordance with the results obtained for a diatomic linear chain of atoms, Similarly, the width of the optical frequency range should be expected to vary as $(\sqrt{1+M_{Be}/M_{ch}}-1)$. However, as the beryllium atom is very much lighter than the chalcogen atoms,
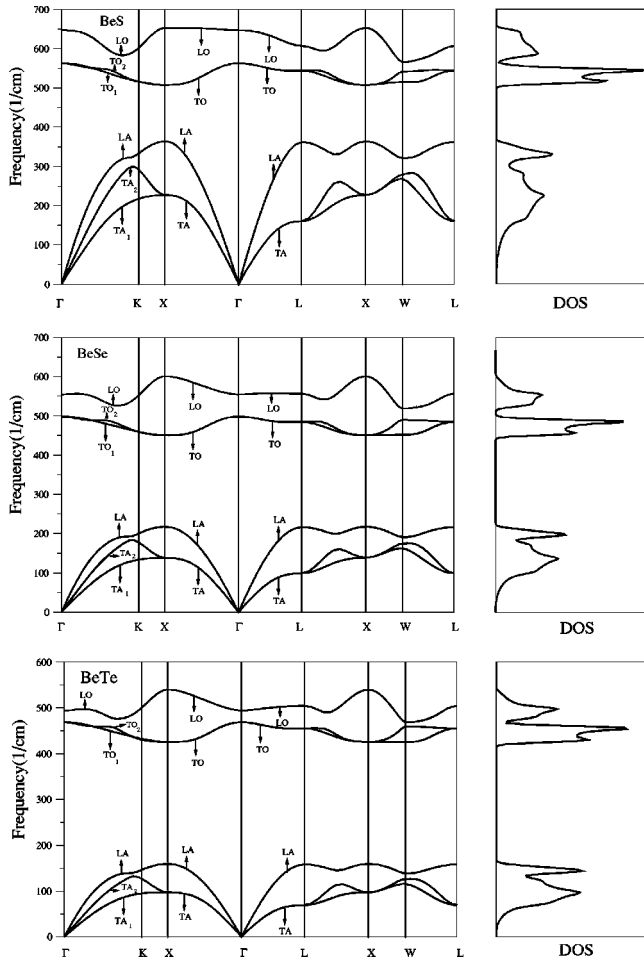
FIG. 2. Calculated phonon dispersions and density of states for Be chalcogenides.

$M_{Be} \ll M_{ch}$, the width of the optical frequency range can be expected to vary as $\sqrt{M_{Be}/M_{ch}}$. These trends are clearly verified from the results of our calculations (cf. Table III). Apart from these obvious trends with regards to the acoustic and optical phonon frequencies, there are three peculiarities in

the dispersion of the longitudinal optical (LO) and transverse optical (TO) branches in these materials.

(i) Along the symmetry direction Γ-X the longitudinal optical (LO) branch is almost flat for BeS, but shows a gradually increasing amount of *upward* dispersion as we move across BeS$\rightarrow$BeSe$\rightarrow$BeTe. Along the Γ-L symmetry direction, the LO branch shows a downward, flat, and upward dispersion for BeS, BeSe, and BeTe, respectively. Along the Γ-K symmetry direction, the dispersion of the LO branch is rather unique, something not observed for other III-V or II-VI semiconductors.

(ii) The LO and TO branches are clearly separated in all materials. The separation between the optical and acoustic regions increases across BeTe, BeSe, and BeS.

(iii) The LO and TO branches do not cross, and at the X symmetry point the LO phonon frequency is significantly higher than the TO phonon frequency for all the three materials.

The third point above requires further discussion and a possible explanation. There are in general two factors which may control the relative positions of the LO and TO frequencies in materials with the zinc-blende and rock salt structures: ionicity and mass ratio. We first remark that the ionicity of Be chalcogenides is comparable to III-V compounds, rather than other II-VI compounds. This is illustrated from a comparison of the pseudocharge density plot along the cation-anion bond for ZnSe, BeTe, and GaAs presented in Fig. 3. Disregarding the 3d peak in the charge density in ZnSe,[20] it is clearly seen that, beyond the midpoint in the bond length and toward the anion, the charge density peak in BeTe is closer to the peak in GaAs (a typical III-V compound) rather than the peak in ZnSe (a typical II-VI compound). Moreover, from an inspection of a wide range of zinc-blende and rock-salt materials, it is clear that there is no direct relationship between the ratio $\omega(TO)/\omega(LO)$ and ionicity[21] (cf. Table IV). We thus conclude that the relative frequencies of the LO and TO modes are more strongly influenced by the mass ratio between the cation and anion.

Table IV lists the ratio of the TO and LO frequencies at the X point, taken from literature, for a few IV-IV, III-V, II-VI, and I-VII materials. It is clearly seen that at the X

TABLE III. Phonon frequencies (in cm^{-1}) calculated at the high-symmetry points Γ, X, and L, for BeS, BeSe, and BeTe. The results are compared with available experimental and theoretical results.

| Material	Reference	TO(Γ)	LO(Γ)	TA(X)	LA(X)	TO(X)	LO(X)	TA(L)	LA(L)	TO(L)	LO(L)
BeS	Present	562	647	237	364	507	652	161	362	543	607
BeSe	Present	498	556	139	218	451	601	99	216	485	556
	Raman[a]	501	579								
	Theory[a]	496	576								
	Theory[b]	501	579	101	252	528	496	72	177	517	538
BeTe	Present	468	495	97	159	425	540	69	158	455	504
	Theory[c]	477									
	Raman[c]	461	502								
	Theory[b]	461	502	80	140	477	468	67	74	473	481

[a]Reference 13.
[b]Reference 11.
[c]Reference 12.
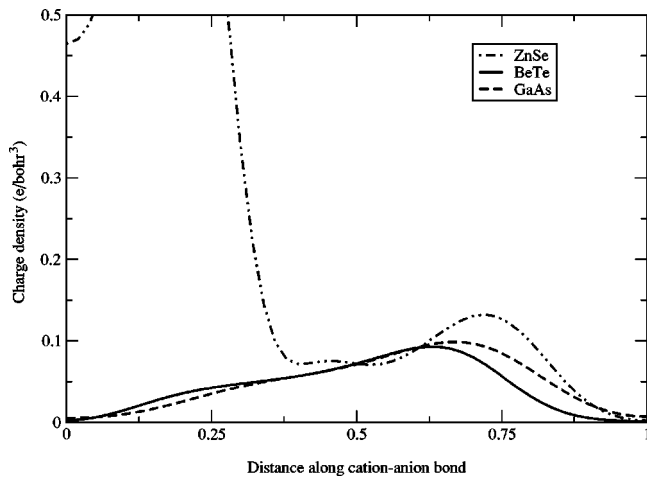
FIG. 3. Pseudocharge density for GaAs, ZnSe, and BeTe, plotted along the bond from the cation site to the anion site.

TABLE IV. Ratio of TO and LO phonon frequencies at the zone edge X for a selected number of IV-IV, III-V, II-VI, and I-VII materials. Also listed are the Phillips ionicity (Ref. 21) of the materials and the mass ratio of the basis atoms.

Material	Mass ratio (cation/anion) or (anion/cation)	Phillips ionicity	$\omega_X(TO)/\omega_X(LO)$
Si	1.0	0.0	1.13
Ge	1.0	0.0	1.14
GaAs	1.07	0.31	1.05
InSb	1.06	0.32	1.13
ZnSe	1.21	0.63	1.44
GaSb	1.74	0.26	1.04
CuBr	1.25	0.73	1.05
AlN	1.93	0.45	0.72
CuI	2.0	0.69	0.86
ZnS	2.04	0.62	0.70
GaP	2.25	0.37	0.92
SiC	2.33	0.18	0.98
BeS	3.56	0.29	0.78
InP	3.71	0.42	0.97
AlSb	4.51	0.36	0.66
GaN	4.98	0.50	0.58
InN	8.20	0.58	0.63
BeSe	8.76	0.26	0.75
BeTe	14.16	0.17	0.79

point the frequency ratio $\omega(TO)/\omega(LO)$ is larger (smaller) than unity for the mass ratio (either cation/anion or anion/cation) smaller (larger) than 2. (The mass ratio of 2 is not a very strong criterion, as the TO/LO frequency ratio at X is slightly smaller than unity for ZnTe for which the mass ratio is 1.95.) From this table it can also be seen that for the same mass ratio, even a large difference between the ionicity factor does not alter this observation. In Be chalcogenides, the mass of the cation (Be) is extraordinarily smaller than the mass of the anion (S, Se, or Te), making the LO mode at X to lie well above the TO mode. We thus hypothesize that the condition $\omega_X(LO) > \omega_X(TO)$ will be satisfied for any zinc-blende or rocksalt material with mass ratio (either cation/anion or anion/cation) larger than approximately 2.0. It should be remarked that diamond (C) and BN are the exceptions to our hypothesis. Although the mass ratio of the basis atoms is much smaller than 2 for both materials (1.0 for C and 1.55 for BN), the frequency $\omega_X(LO)$ is higher than $\omega_X(TO)$. This out-of-trend behavior is most probably due to the combined effects of short bond length and strong localization of electronic charge close to the basis atoms in diamond and close to N in BN.

Our calculated values of the zone-center LO and TO frequencies compare very well with the Raman scattering measurements reported by Wagner *et al.*,[13] and the theoretical

results presented in the works by Wagner *et al.*[13] and Doyen-Lang.[11] However, the dispersion of the LO and TO branches obtained in the theoretical works by Doyen-Lang *et al.* and by Wagner *et al.*[13] are hugely different from the predictions made in the present first-principles work. It should be pointed out that the phonon dispersion curves for BeSe and BeTe calculated by Doyen-Lang *et al.*[11] are based on the application of the simple force constant model due to De Launey. On the other hand, Wagner *et al.*[13] employed a linear chain model to sketch the phonon dispersion branches in BeTe. While the force constant parameters in their theoretical works have been fitted to reproduce the spectroscopic measurements for the zone-center LO and TO modes, the
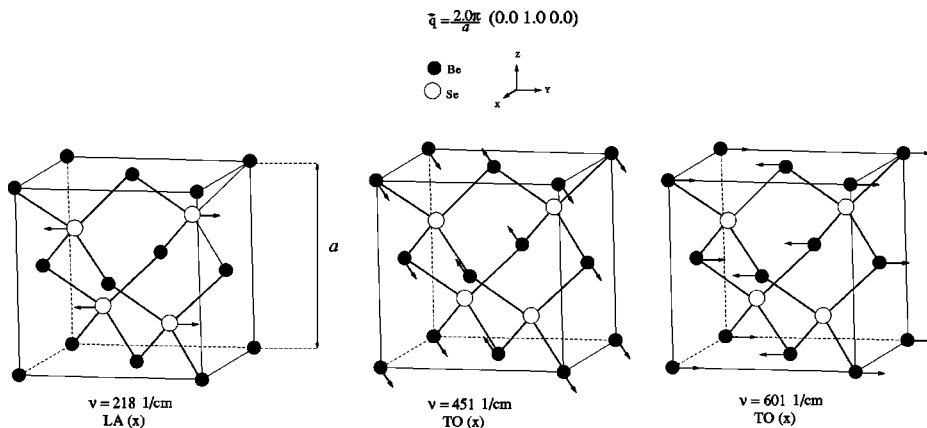
$$\bar{q} = \frac{2.0\pi}{a} (0.0\ 1.0\ 0.0)$$

FIG. 4. Schematic illustration of the eigen displacements of LA, TO, and LO phonon modes for BeSe at the X point.

simple lattice dynamical models employed are clearly inadequate to reproduce the correct dispersions of the LO and TO branches. In particular, the crossing of the LO and TO branches in the works by Doyen-Lang *et al.*[11] and Wagner *et al.*[13] suggests that the lattice dynamics of BeSe follows the trend for ZnSe. Our work, on the other hand, suggests that the lattice dynamics of BeSe follows the trend in ZnS, not ZnSe. This can be understood by noting that the mass differences between two ions is much larger in BeSe and ZnS than in ZnSe.

The atomic displacement patterns from our calculations at the zone-edge point X are shown in Fig. 4. The longitudinal acoustic (LA) mode corresponds to the motion of the heavier atom (S, Se, or Te), while the LO and TO modes result from the motion of the Be atom in all the three materials. These results are in general true for the vibrational eigenvectors in all III-V semiconductors in the zinc-blende phase.[23]

IV. SUMMARY

In this paper, we have investigated the structural, electronic and dynamical properties of the beryllium compounds BeS, BeSe, and BeTe by employing a first-principles scheme, based on the application of the plane-wave pseudopotential method, density functional theory, and a linear response technique. The calculated static properties, viz. equilibrium lattice constant a, bulk modulus B, and pressure derivative of bulk modulus B' are in agreement with previous theoretical and available experimental results. Our study yields an indirect band gap with the minimum of the conduction band at the X point for all three compounds. In particular, the calculated electronic structure for BeTe shows very good agreement with experimental results for the top valence bands along the Γ-X direction. The dispersion of the LO and TO branches in these materials are found to be different from many studied I-VI, II-VI, III-V, and IV-IV materials. In these materials the TO branch in general lies below the LO branch. In particular, due to the huge mass difference between Be and the chalcogens, at the Brillouin zone edge X the frequency of the TO mode is significantly lower than the frequency of the LO mode. We have hypothesized that the condition $\omega_X(\text{LO}) > \omega_X(\text{TO})$ will be satisfied for materials with the zinc-blende or rocksalt structure with the mass ratio (either cation/anion or anion/cation) larger than approximately 2.

[1] D. J. Stukel, Phys. Rev. B **2**, 1852 (1970).

[2] Ch. Verie, in *Proceedings of the International Conference on Heteroepitaxy Growth, Characterization and Device Applications*, edited by B. Gill and R.-L. Aulombaud (World Scientific, Singapore, 1995), p. 73.

[3] A. Munoz, P. Rodriguez-Hernandez, and A. Mujica, Phys. Rev. B **54**, 11861 (1996).

[4] A. Munoz, P. Rodriguez-Hernandez, and A. Mujica, Phys. Status Solidi B **198**, 439 (1996).

[5] P. E. Van Camp and V. E. Van Doren, Solid State Commun. **98**, 741 (1996).

[6] A. Waag, F. Fischer, H. J. Lugauer, T. Litz, J. Laubender,U. Lunz, U. Zhender, W. Ossau,T. Gerhardt, M. Moller, and G. Landhehr, J. Appl. Phys. **80**, 792 (1996).

[7] M. Gonzalez-Diaz, P. Rodriguez-Hernandez, and A. Munoz, Phys. Rev. B **55**, 14043 (1997).

[8] M. Nagelstraβer, H. Dröge, H. P. Steinrück, F. Fischer, T. Litz, A. Waag, G. Landwehr, A. Fleszar, and W. Hanke, Phys. Rev. B **58**, 10394 (1998).

[9] N. Benosman, N. Amrane, S. Meçabih, and H. Aourag, Physica B **304**, 214 (2001).

[10] J. De Launay, Solid State Phys. **3**, 203 (1957).

[11] S. Doyen-Lang, O. Pages, L. Lang, and J. Hugel, Phys. Status Solidi B **229**, 563 (2002).

[12] V. Wagner, S. Gundel, J. Geurts, T. Gerhard, Th. Litz, H-J. Lugauer, F. Fischer, A. Waag, G. Landwehr, R. Kruse, Ch. Becker, and U. Küster, J. Cryst. Growth **184/185**, 1067 (1998).

[13] V. Wagner, J. J. Liang, R. Kruse, S. Gundel, M. Kleim, A. Waag, and J. Geurts, Phys. Status Solidi B **215**, 87 (1999).

[14] N. Troullier and J. L. Martins, Phys. Rev. B **43**, 1993 (1991).

[15] D. M. Ceperly and B. J. Alder, Phys. Rev. Lett. **45**, 566 (1980); J. Perdew andA. Zunger, Phys. Rev. B **23**, 5048 (1981).

[16] D. J. Chadi and M. L. Cohen, Phys. Rev. B **8**, 5747 (1973).

[17] S. Baroni, S. de Gironcoli, A. Dal Corso, and P. Giannozzi, Rev. Mod. Phys. **73**, 515 (2001).

[18] P. Villars and L. D. Calvert, *Pearson's Handbook of Crystallographic Data for Intermetallic Phases* (American Society of Metals, Metals Park, OH, 1985).

[19] G. P. Srivastava, *Theoretical Modeling of Semiconductor Surfaces* (World Scientific, Singapore, 1999).

[20] The 3*d* electrons in the Zn atom were considered as a part of the active valence shell. This produces a peak in the charge density close to the Zn ion. For the purpose of the comparison of the charge density along the cation-anion bond with BeTe and GaAs this peak in ZnSe should be disregarded.

[21] J. C. Phillips, *Bonds and Bands in Semiconductors* (Academic, New York, 1973).

[22] H. M. Tütüncü and G. P. Srivastava, Phys. Rev. B **62**, 5028 (2000).

[23] P. Giannozzi, S. de Gironcoli, P. Pavone, and S. Baroni, Phys. Rev. B **43**, 7231 (1991).

[24] *Semiconductors. Others than Group IV Elements and III-V Compounds*, edited by O. Madelung, Data in Science and Technology Series, Vol. VIII (Springer-Verlag, Berlin, 1992).

[25] H. Luo, K. Ghandehari, R. G. Greene, A. L. Ruoff, S. S. Trail, and F. J. DiSalvo, Phys. Rev. B **52**, 7058 (1995).